ELECTROANALYSIS

Electrochemical detection of asparaginase antibodies using bifunctionalized carbon interfaces

Daisy Marshall | Joshua Lehr [ID]

School of Science, Engineering and
Environment, University of Salford,
Salford, United Kingdom

Correspondence
Joshua Lehr, School of Science,
Engineering and Environment,
University of Salford, 43 Crescent,
Salford, M5 4WT, United Kingdom.
Email: j.lehr@salford.ac.uk

Abstract

The early detection of anti-asparaginase biomarker can facilitate timely modification of asparaginase chemotherapy, thereby avoiding serious complications. Herein we describe the preparation of a novel electrochemical biosensing interface for rapid detection of anti-asparaginase in the picomolar range (1–10000 pM). Coimmobilization of ferrocene and asparaginase on a carbon interface (via diazonium grafting) facilitates transduction through attenuation of the surface-bound ferrocene redox couple. The limit of detection of 0.8 pM for this point-of-care applicable method compares favourably to that of traditional faradaic assaying (2.0 pM) where transduction occurs by the target blocking the diffusion of the solution redox probe $[Fe(CN)_6]^{3-/4-}$.

KEYWORDS
anti-asparaginase, asparaginase, biosensor, diazonium, leukaemia

Acute lymphoblastic leukaemia (ALL) is a cancer most commonly found in children [1]. Current treatments generally involve multidrug chemotherapy regimens incorporating the drug L-asparaginase. [2] Unfortunately, L-asparaginase treatment can cause acute side effects, including hypersensitivity and anaphylactic shock. The latter is a particularly serious concern. Anti-asparaginase is usually present in the patient's blood several days prior to the occurrence of the anaphylactic shock. [3] There is also some evidence that high anti-asparaginase levels are associated with less effective treatment. Hence, monitoring of anti-asparaginase levels can not only facilitate early detection of adverse reaction to the drug, but also underpin early evaluation of treatment effectiveness, thereby enabling timely and appropriate changes to the chemotherapy regimen [2b, 4].

Anti-asparaginase detection/quantification is traditionally undertaken using enzyme-linked immunosorbent assay (ELISA) [5]. While ELISAs are highly sensitive and reliable, and the current clinical "gold standard" for protein biomarker detection, they do suffer from a number of drawbacks. They require specialist laboratories with trained technicians and thus cannot be used for point-of-care (POC) and continuous/high-frequency monitoring. Electrochemical biosensors overcome these limitations by offering the possibility of low-cost, miniaturized, rapid, POC monitoring for prognostics [6]. Electrochemical protein biomarker detection is generally based on immobilisation of a target-complementary recognition site (e.g. antigen, antibody, aptamer, etc) on an electrode interface. Target binding to the recognition site can be monitored by measuring the inhibition of charge transfer from a redox-active diffusive species [7], subtle changes in the non-faradaic characteristics of the surface [8], or by attenuation of the signal from a surface-incorporated redox probe [9]. The first of these methodologies, often referred to as the "faradaic" approach, has been extensively reported and leads to sensitive detection. However, since the redox probe must be added to the sampling solution, it offers only limited advantages over ELISA and is not suitable for POC applications. The latter methodologies, namely the "non-faradaic" and "surface-faradaic", are approaches that could facilitate true POC monitoring by eliminating the need for complicated sample preparation. Such approaches have significant potential applications in

diagnostics/prognostics and could be used to underpin, for example, the rapid, POC, monitoring of anti-asparaginase levels.

Herein, we report a novel surface-faradaic anti-asparaginase biosensor prepared by co-immobilisation of a redox-active ferrocene group and an asparaginase receptor on a carbon electrode interface. While some previous electrochemical surface-faradaic protein biomarker sensors have been prepared on gold [9], carbon is an attractive substrate for electrochemical biosensors, offering a low cost, biocompatible, and robust interface. Unlike gold, carbon is not prone to etching from CN^- and Cl^- anions that will often be present during sensor construction and use [7]. Furthermore diazonium chemistry offers a simple route to highly stable layers on carbon [10]. As a result there has been interest in the application of diazonium chemistry to the development of biosensors [11]. The formation of mixed bifunctional layers is also accessible via diazonium chemistry [12]. Consequently, we have prepared bifunctional carboxy/azide terminated layers on glassy carbon interfaces by diazonium electrografting. Sequential attachment of the ferrocene transducer and the asparaginase recognition site onto this primer layer then underpinned selective detection of anti-asparaginase in the picomolar range. The method was compared to traditional faradaic assaying on the same interfaces. The strategy for sensor construction reported herein is outlined in Scheme 1.

Sensor construction – Grafting of the mixed phenyl azide (PA)/phenylacetic acid (PAA) film was undertaken by carrying out reductive voltammetric scans in a mixture of the corresponding in-situ generated diazonium cations (Scheme 1, step 1), as described in the experimental section. On the first scan a single reduction peak was observed at -0.59 V vs. SCE (Figure 1a) consistent with the electrochemical reduction and grafting of the two diazonium components (individually observed at approximately -0.59 V vs. SCE, Figure SI 1). On repeat scans this peak was not observed, indicative of the formation of a passivating film on the electrode surface.

Grafting of the bifunctional PA/PAA layer was also accompanied by a loss of diffusive $[Fe(CN)_6]^{3-/4-}$ voltammetric signal (Figure SI 2) and an increase in the associated charge transfer resistance (R_{ct}) from ~2 kΩ to ~1.0 MΩ as expected for a electrochemical blocking film (Figure 1b). Evidence for the formation of a mixed film incorporating both PA and PAA functionalities can be found by comparing the $[Fe(CN)_6]^{3-/4-}$ response from a layer grafted with both components, to those grafted from only a single component. The R_{ct} value of ~1.0 MΩ for the mixed layer was found to be lower than that of the highly blocking (negatively charged) single component PAA layer (~1.7 MΩ) and higher than that of the
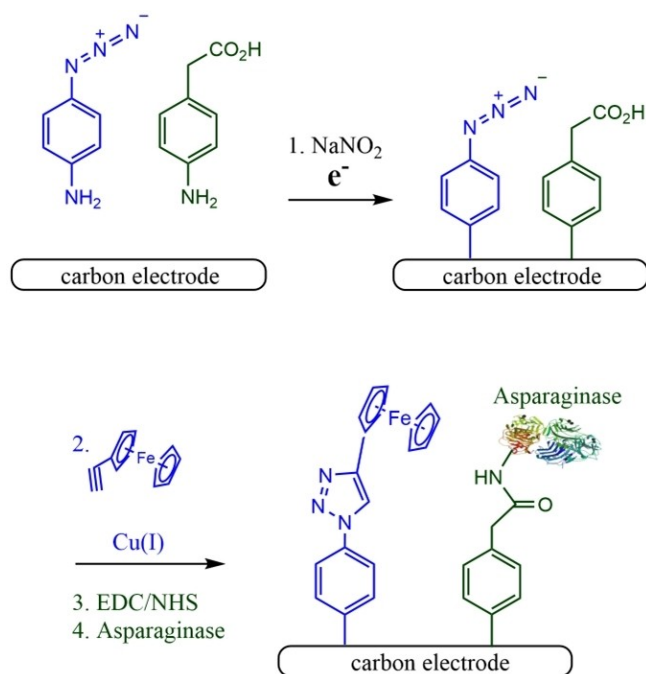
SCHEME 1 Schematic showing strategy for the construction of the sensing interface. Step 1: electrochemical grafting of bifunctional phenyl azide (PA)/ phenylacetic acid (PAA) film from diazonium cations generated in-situ from the corresponding aryl amines. Step 2: attachment of ferrocene moiety by copper(I) catalyzed azide–alkyne cycloaddition (CuAAC) to the PA functionality. Step 3: Activation of the PAA functionality. Step 4. Coupling of asparaginase to the activated acid by peptide bond formation.

(net neutral) PA layer (~75 kΩ), consistent with the formation of the bifunctional (mixed) film (Figure SI 3).

Attachment of ferrocene to the bifunctional films was achieved by copper(I) catalyzed azide–alkyne cycloaddition (CuAAC), as described in the experimental section (Scheme 1, step 2). The electrodes were then transferred into a cell containing 0.2 M $NaClO_4$ and the expected ferrocene/ferrocenium (Fc/Fc^+) redox couple was observed at $E_{1/2} = 0.31$ V vs. SCE (Figure 1c). When the CuAAC reaction was carried out without sodium ascorbate (needed to form the relevant Cu(I) catalyst species) no Fc/Fc^+ signal was observed, indicating chemical specificity of the surface CuAAC reaction and confirming that the observed couple is not associated with the Cu^+/Cu^{2+} redox system. A linear relationship between peak current and scan rate further confirms the ferrocene is surface bound (Figure SI 4). The charge associated with the Fc/Fc^+ redox couple was determined as ~1.0 μC - corresponding to a surface concentration of ferrocene groups of $\Gamma_{Fc} \approx 3.4 \ 10^{-10}$ mol cm^{-2} and indicating sub-monolayer concentrations of ferrocene on the surface (a tightly packed monolayer of ferrocene is ~5.8×10^{-10} mol cm^{-2}) [13]. This is expected for covalent
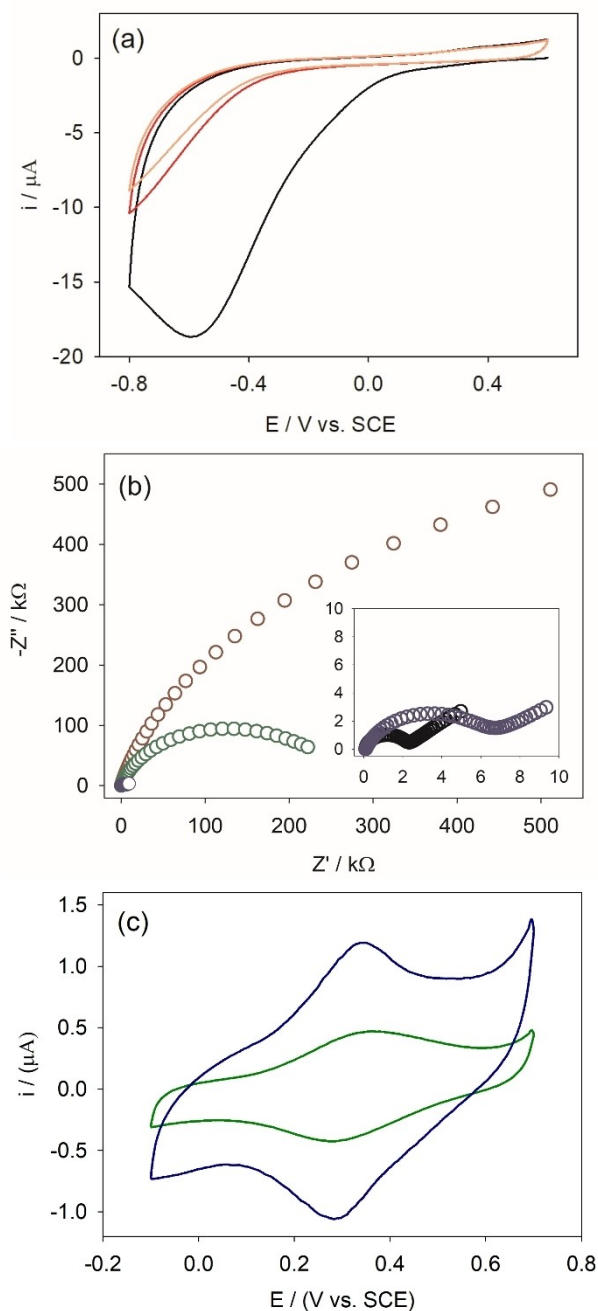
FIGURE 1 (a) Cyclic voltammograms of GC working electrode in 2.5 mM 4-azido aniline, 2.5 mM 4-aminophenylacetic acid, and 5 mM NaNO$_2$ in 0.5 M HCl. First scan (black), second scan (red) third scan (orange). (b) EIS spectra (Nyquist plots) recorded in 2 mM [Fe(CN)$_6$]$^{3-/4-}$ in 0.2 M NaClO$_4$ at a bare electrode (black) and after grafting of a mixed PA/PAA film (red), subsequent attachment of ferrocene by click reaction (blue) and further attachment of asparaginase by peptide bond formation (green). (c) Cyclic voltammograms of GC electrodes after ferrocene attachment showing the surface bound ferrocene/ferrocenium (Fc/Fc$^+$) redox couple in 0.2 M NaClO$_4$ before (blue) and after (green) attachment of the asparaginase recognition site.

attachment to bifunctional diazonium derived films, where specific attachment sites are spaced/diluted across the surface in an already loosely packed film [14]. As a comparison, a single component PA film yielded $\Gamma_{Fc} \approx 4.3 \times 10^{-10}\,mol\,cm^{-2}$ after CuAAC reaction, higher than when both components are used, as expected. Interestingly, the R_{ct} to [Fe(CN)$_6$]$^{3-/4-}$ in solution was seen to decrease to ~6 kΩ following CuAAC "click" coupling of ferrocene to the interface, possibly due to redox mediation of [Fe(CN)$_6$]$^{3-/4-}$ electron transfer by the surface bound ferrocene moiety [15]. Alternatively this observation could also be attributed to the more neutral interface resulting from reaction of the (doubly) charged N$_3$ terminus.

Further evidence for the attachment of ferrocene to the mixed PA/PAA films was obtained from x-ray photoelectron spectroscopy (XPS). Scans in the N1s region showed peaks at 405 and 400 eV, indicative of the presence of azide on the GC interface. Subsequent CuAAC reaction saw the disappearance of the peak at ~405 eV, consistent with the formation of the triazole group and successful click reaction [16]. Furthermore scans in the Fe2p region after the CuAAC reaction showed peaks at 720 and 708 eV, assigned to the Fe2p$_{1/2}$ and Fe2p$_{3/2}$ signals of Fe^{2+}, respectively, and are indicative of the presence of ferrocene on the interface [17] (Figure SI 5).

After attachment of the ferrocene moiety, the asparaginase recognition site was attached to the interface by EDC/NHS activation of the PAA sites and subsequent peptide bond formation with the asparaginase (Scheme 1, step 4), as described in the experimental section. Attachment of the asparaginase was accompanied by the expected increase in R$_{ct}$ (from ~6 kΩ to ~210 kΩ, Figure 1b). A decrease in the charge associated with the Fc/Fc$^+$ couple (from ~1.0 μC to ~0.6 μC, Figure 1c) was also observed and can be attributed to decreased electrolyte access or change in local dielectric around the ferrocene after protein coupling [9]. Neither of these effects were observed upon immersion of the electrodes in asparaginase without prior EDC/NHS activation, indicating the chemical specificity of the peptide bond formation is responsible for the observed changes.

Assaying – After preparation of the ferrocene/asparaginase sensing interfaces, voltammograms of the sensing electrodes, recorded in the absence of anti-asparaginase target, showed a stable Fc/Fc$^+$ couple upon repeat scans with negligible change in Fc/Fc$^+$ charge. Upon subsequent immersion in increasing concentrations of anti-asparaginase target, attenuation of the Fc/Fc$^+$ redox system was observed (Figure 2a). The
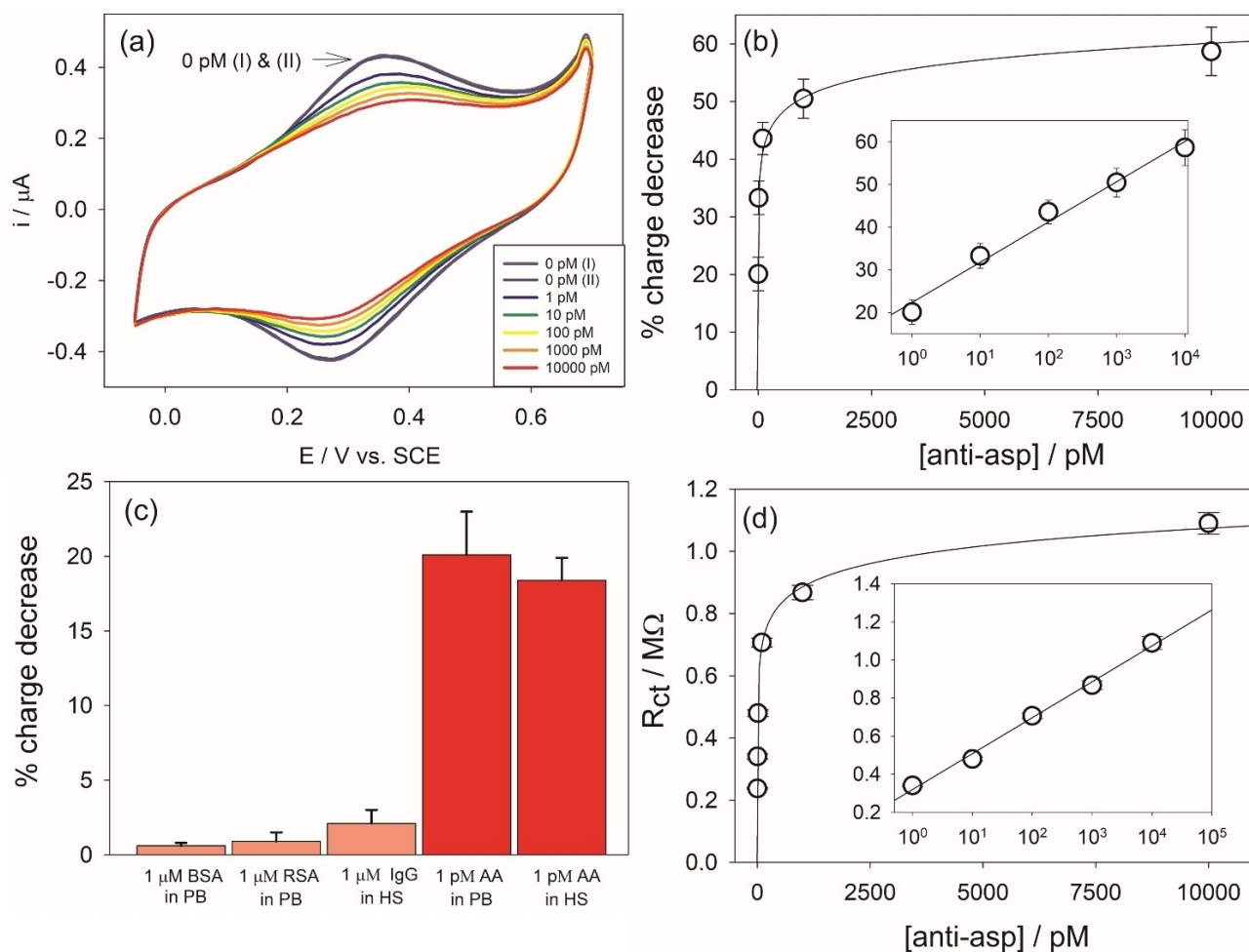
FIGURE 2 (a) Cyclic voltammetric response of the ferrocene/asparaginase modified interfaces showing attenuation of the Fc/Fc$^+$ couple upon immersion in increasing concentration of the target anti-asparaginase. (b) Analytical curve showing percentage charge decrease for the Fc/Fc$^+$ redox couple of the ferrocene/asparaginase modified sensing interfaces upon immersion in increasing concentration of anti-asparaginase (n = 4). Errors calculated from the standard deviation from the eight charge measurements across the four samples (one anodic and one cathodic charge for each sample). (c) Controls, in phosphate buffer (PB) and 20% human serum (HS), comparing the relative sensor response to 1×10^6 pM (1 μM) of non-specific proteins (BSA, RSA and naturally occurring human IgG) to 1 pM of the target (anti-asparaginase, AA). (d) Analytical curve showing change in R_{ct} to $[Fe(CN)_6]^{3-/4-}$ of the ferrocene/asparaginase electrodes upon immersion in increasing concentrations of target anti-asparaginase.

attenuation is attributed to a change in the dielectric around the ferrocene moiety, or inhibition of electrolyte diffusion to the moity, upon target binding. [9] The resulting analytical curve (Figure 2b) shows a response between 1–10000 pM of target with a limit of detection (LOD) = 0.8 pM.

Although the clinically relevant anti-asparaginase concentration range for detection of asparaginase hypersensitivity has not been reported explicitly in terms of molecular concentration, some rationalizations can be made. Considering a conservative (low) LOD for ELISA of approximately 2 fM [18] and that the detection of asparaginase hypersensitivity by anti-asparaginase ELISA at 1:10000 dilution has been reported [19], it follows that a sensor with an LOD in the low pM range (i.e.

below 20 pM) would comfortably detect anti-asparaginase concentrations associated with asparaginase hypersensitivity. Furthermore, previous work has reported detection of asparaginase hypersensitivity in clinical samples using surface plasmon resonance configuration with an LOD of 500 pM [3]. Hence, the current sensing system comfortably falls within the clinically useful range.

The sensing interfaces' selectivity was also assessed (Figure 2c). Specifically, the response of the sensing electrodes to non-specific proteins, namely bovine serum albumin (BSA) and rabbit serum albumin (RSA), at a million times the lowest measured concentration of the target, was negligible - and well below the response associated with the LOD. Similarly the response from

naturally occurring human IgG in 20% human serum was also negligible. On the other hand, significant response was seen from 1 pM of the target anti-asparaginase in 20% serum. These experiments indicate a high level of specificity of the sensing interface.

On selected electrodes the recruitment of the anti-asparaginase target to the interface was also followed by faradaic EIS in the presence of $[Fe(CN)_6]^{3-/4}$. Figure 2d shows that a quantitative response to target binding on the ferrocene/asparaginase electrodes is also observed using this traditional sensing strategy. The response from faradaic $[Fe(CN)_6]^{3-/4}$ EIS is seen to have a comparable concentration-response profile to that from the Fc/Fc^+ couple, consistent with the same interaction being responsible for both responses. The LOD from faradaic EIS detection was determined to be 2.0 pM – this is comparable (though slightly higher) to that from the Fc/Fc^+ surface bound couple and provides an interesting comparison of the sensitivities of the two methods.

Hence, herein we have reported the preparation of a sensing architecture based on a carbon interface bifunctionalized using diazonium chemistry to incorporate a receptor (asparaginase) alongside redox reporter (ferrocene). Using the surface bound ferrocene redox reporter, selective detection of anti-asparaginase in a range of 1–10000 pM and with LOD of 0.8 pM was achieved. This was shown to be comparable (slightly lower) than the LOD of 2.0 pM achieved using traditional diffusive faradaic sensing at the same interface. Importantly the surface redox approach (unlike the diffusive faradaic approach) is applicable to POC prognostics. The detection range and LOD appears within clinically relevant values. The approach could be developed for monitoring of leukaemia patients undergoing asparaginase treatment, thereby underpinning early detection of adverse effects of treatment. The overall strategy can also, in principle, be applied to other prognostic and diagnostic challenges.

EXPERIMENTAL

All chemicals were purchased from Sigma-Aldrich unless stated otherwise. Anti-asparaginase was purchased from Cell Signalling Technology. Aqueous solutions were prepared with milli Q water (≥ 18.2). All electrochemistry was carried out using PalmSens4 potentiostat with a three-electrode cell incorporating a glassy carbon (GC) disc working electrode (CHI, d = 3 mm), a platinum wire counter electrode and a saturated calomel electrode (SCE) as a reference electrode. Electrochemical impedance spectroscopy (EIS) was carried out in aqueous solutions containing 2 mM potassium ferricyanide

($[Fe(CN)_6]^{3-/4-}$) and 0.2 M $NaClO_4$ supporting electrolyte, in the frequency range of 0.1–100 000 Hz with an amplitude of 10 mV at the half wave potential of the $[Fe(CN)_6]^{3-/4-}$ redox couple. Voltammetry was analyzed using PStrace, while EIS spectra were fitted to a Randles Circuit using EIS spectrum analyser to determine the charge transfer resistance (R_{ct}).

Grafting of bifunctional (mixed) phenyl azide (PA) / phenylacetic acid (PAA) layers was undertaken using insitu diazonium grafting methodology [20]. Cyclic voltammetric scans were carried out at GC working electrodes between +0.6 and −0.8 V vs. SCE in a solution of 2.5 mM 4-azidoanaline, 2.5 mM 4-aminophenylacetic acid, and 5 mM $NaNO_2$ in 0.5 M HCl. Monofunctional (single component) reference interfaces were grafted using the same conditions with 5 mM of the single precursor aryl amine. After grafting of the bifunctional layer, copper(I) catalyzed azide-alkyne cycloaddition (CuAAC) was undertaken by immersion of the functionalized electrodes in 1:1 v:v of water:isopropyl alcohol containing 5 mM ethynylferrocene, 1 mM copper (II) sulphate and 2 mM sodium ascorbate, for 20 hours. Subsequently the electrodes were washed and sonicated in water and isopropyl alcohol prior to electrochemical analysis. Attachment of the asparaginase was undertaken by activation of the PAA functionality in aqueous solution containing 0.4 M EDC and 0.1 M NHS for 40 minutes followed by transfer to a solution of 5 μM asparaginase in 0.01 M phosphate buffer (pH = 7.4). Thereafter, the electrodes were washed with distilled water and suspended in 10 mM lysine in 0.01 M phosphate buffer (pH = 7.4) for 30 minutes to block any unreacted activated sites with an antifouling (zwitterionic) functionality. The construction of the electrode sensing interfaces was followed by voltammetry and EIS after each step.

Prior to assaying all sensing interfaces were cycled to ensure a stable ferrocene/ferrocenium (Fc/Fc^+) redox system with 10 min intervals between. Assaying was carried out by immersing the sensing electrodes in solutions of increasing concentration of anti-asparaginase (1–100000 pM) in 0.1 M phosphate buffer (pH = 7.4) for 10 minutes and recording voltammograms of the Fc/Fc^+ redox system. Target binding was also followed by recording $[Fe(CN)_6]^{3-/4-}$ impedance spectra (as described above) after each concentration for selected interfaces. This was undertaken with selected interface only to verify it did not interfere with the Fc/Fc^+ response. Controls involving non-specific proteins were carried out under the same conditions, and with the same immersion times, as the sample measurements on electrodes prior to addition of target protein.

X-ray Photoelectron Spectroscopy (XPS) was performed using an ESCA2SR spectrometer (ScientaOmicron

GmbH) using monochromated Al Kα radiation (1486.6 eV, 20 mA emission at 300 W, 1 mm spot size) with a base vacuum pressure of ~1×10^{-9} mbar. Charge neutralisation was achieved using a low energy electron flood source (FS40 A, PreVac). Binding energy scale calibration was performed using C−C in the C 1s photoelectron peak at 285 eV. Analysis and curve fitting was performed using Voigt-approximation peaks using CasaXPS.

CONFLICT OF INTEREST STATEMENT
The authors declare no conflicts of interest.

DATA AVAILABILITY STATEMENT
Data available on request from the authors.

ORCID
Joshua Lehr http://orcid.org/0000-0001-5698-7244

REFERENCES
1. a) A. Miranda-Filho, M. Piñeros, J. Ferlay, I. Soerjomataram, A. Monnereau, F. Bray, *Lancet Haematol* **2018**, *5*, e14-e24; b) T. Terwilliger, M. Abdul-Hay, *Blood Cancer J* **2017**, *7*, e577-e577.
2. a) V. I. Avramis, P. N. Tiwari, *Int. J. Nanomed.* **2006**, *1*, 241–254; b) D. K. Cecconello, M. R. d. Magalhães, I. C. R. Werlang, M. L. d. M. Lee, M. B. Michalowski, L. E. Daudt, *Hematol. Transfus. Cell Ther* **2020**, *42*, 275–282.
3. A. Aubé, D. M. Charbonneau, J. N. Pelletier, J.-F. Masson, *ACS Sens.* **2016**, *1*, 1358–1365.
4. J. Paillassa, T. Leguay, X. Thomas, F. Huguet, M. Audrain, V. Lheritier, C. Vianey-Saban, C. Acquaviva-Bourdain, C. Pagan, H. Dombret, N. Ifrah, N. Boissel, M. Hunault-Berger, *Blood Cancer J* **2018**, *8*, 45–45.
5. C. Liu, J. D. Kawedia, C. Cheng, D. Pei, C. A. Fernandez, X. Cai, K. R. Crews, S. C. Kaste, J. C. Panetta, W. P. Bowman, S. Jeha, J. T. Sandlund, W. E. Evans, C. H. Pui, M. V. Relling, *Leukemia* **2012**, *26*, 2303–2309.
6. S. Campuzano, M. Pedrero, P. Yáñez-Sedeño, J. M. Pingarrón, *Sens. Actuators B* **2021**, *345*, 130349.
7. V. Pinkova Gajdosova, L. Lorencova, A. Blsakova, P. Kasak, T. Bertok, J. Tkac, *Curr. Opin. Electrochem.* **2021**, *28*, 100717.
8. Q. Xu, H. Cheng, J. Lehr, A. V. Patil, J. J. Davis, *Anal. Chem.* **2015**, *87*, 346–350.
9. a) C.-Y. Chen, J. Lehr, *Electroanalysis* **2021**, *33*, 563–567; b) J. Lehr, F. C. Bedatty Fernandes, P. R. Bueno, J. J. Davis, *Anal. Chem.* **2014**, *86*, 2559–2564.
10. a) J. Pinson, F. Podvorica, *Chem. Soc. Rev.* **2005**, *34*, 429–439; b) A. J. Downard, *Electroanalysis* **2000**, *12*, 1085–1096.
11. D. Hetemi, V. Noël, J. Pinson, *Biosensors* **2020**, *10*, 4.
12. C. Jiang, S. Moraes Silva, S. Fan, Y. Wu, M. T. Alam, G. Liu, J. Justin Gooding, *J. Electroanal. Chem.* **2017**, *785*, 265–278.
13. L. Y. S. Lee, T. C. Sutherland, S. Rucareanu, R. B. Lennox, *Langmuir* **2006**, *22*, 4438–4444.
14. a) P. A. Brooksby, A. J. Downard, *Langmuir* **2004**, *20*, 5038–5045; b) J. Lehr, B. E. Williamson, A. J. Downard, *J. Phys. Chem. C* **2011**, *115*, 6629–6634.
15. O. Azzaroni, M. Álvarez, M. Mir, B. Yameen, W. Knoll, *J. Phys. Chem. C* **2008**, *112*, 15850–15859.
16. A. E. Daugaard, S. Hvilsted, T. S. Hansen, N. B. Larsen, *Macromolecules* **2008**, *41*, 4321–4327.
17. Y. Yokota, Y. Mino, Y. Kanai, T. Utsunomiya, A. Imanishi, M. A. Wolak, R. Schlaf, K.-i. Fukui, *J. Phys. Chem. C* **2014**, *118*, 10936–10943.
18. S. Zhang, A. Garcia-D'Angeli, J. P. Brennan, Q. Huo, *Analyst* **2014**, *139*, 439–445.
19. B. Wang, L. J. Hak, M. V. Relling, C. H. Pui, M. H. Woo, M. C. Storm, *J. Immunol. Methods* **2000**, *239*, 75–83.
20. S. Baranton, D. Bélanger, *J. Phys. Chem. B* **2005**, *109*, 24401–24410.

SUPPORTING INFORMATION
Additional supporting information can be found online in the Supporting Information section at the end of this article.

Graphical Abstract

The contents of this page will be used as part of the graphical abstract of html only.
It will not be published as part of main.